

# Low-resistance nonalloyed ohmic contacts to Si-doped molecular beam epitaxial GaAs

P. D. Kirchner, T. N. Jackson, G. D. Pettit, and J. M. Woodall  
IBM T.J. Watson Research Center, Yorktown Heights, New York 10598

(Received 4 March 1985; accepted for publication 8 April 1985)

We have found evidence that the surface depletion charge density in molecular beam epitaxial *n*-GaAs doped heavily with Si approaches the Si concentration. *In situ* metallization of the as-grown surface of GaAs uniformly doped with Si at  $1 \times 10^{20} \text{ cm}^{-3}$  yields a specific contact resistivity of  $1.3 \mu\Omega \text{ cm}^2$ , indicating a space-charge density about equal to the silicon density despite a measured bulk electron density of  $4 \times 10^{18} \text{ cm}^{-3}$ . This contact resistivity is among the lowest for nonalloyed ohmic contacts to *n*-GaAs. We attribute the large discrepancy between surface space-charge density and bulk electron density to the amphoteric behavior of silicon in GaAs. Surface Fermi-level pinning and arsenic stabilization create a surface depletion region where donor site selection predominates, whereas the extrinsic electron density in the bulk causes self-compensation.

Bulk thermochemistry establishes that for a given crystal growth condition, an amphoteric dopant such as silicon in GaAs has an equilibrium ratio of donors to acceptors that is proportional to the ratio of holes to electrons.<sup>1</sup> Consequently, carrier density saturates at high dopant concentrations by causing the ratio of donors to acceptors to approach unity. However, in GaAs, a wide variety of conditions pins the surface Fermi level near midgap, depleting the near-surface region of free carriers and fixing the hole-to-electron ratio there near unity. Thus, if Fermi-level pinning occurs at the surface during growth, the equilibrium donor-to-acceptor ratio in the surface depletion region does not depend upon dopant concentration, and saturation of the surface space-charge density should not occur. This is important because most metal contacts to GaAs produce midgap pinning which, in order to exhibit low-resistance ohmic behavior, requires the depleted GaAs at the metal interface to have a high space-charge density.

In this letter, we report that for molecular beam epitaxy (MBE) of (100) GaAs doped with Si, measured bulk electron concentrations and surface space-charge densities that are inferred through contact resistance indicate that initial selection of donor and acceptor sites by Si atoms is dominated by the effects of arsenic stabilization and the consequent Fermi-level pinning. *In situ* metallization of GaAs doped with Si at  $1 \times 10^{20} \text{ cm}^{-3}$  yields a specific contact resistivity of  $1.3 \mu\Omega \text{ cm}^2$  at 300 K. The solubility limit of Si in GaAs of  $\sim 2 \times 10^{20} \text{ cm}^{-3}$  (Ref. 2) suggests that a contact resistivity as low as  $0.5 \mu\Omega \text{ cm}^2$  might be achieved.

Molecular beam epitaxial GaAs doped with Si was grown with elemental sources at a growth rate of  $1 \mu/\text{h}$  using semi-insulating (100) GaAs substrates held at 550–610 °C with  $\text{As}_4$  or  $\text{As}_2$  pressures roughly ten times the Ga pressure. Silicon was sublimed from an etched silicon wafer with many parallel filaments.<sup>3</sup> Electrically, the source resembles the single filament used by Miller and co-workers,<sup>4,5</sup> because thermal runaway causes only one filament to heat. This source allows high-purity Si doping at high growth rates. For growth of GaAs at micron-per-hour rates, the conventional Si effusion cell is unsuitable for doping at percent levels, because the high temperatures required decompose its

boron nitride crucible and insulators.

The layers were doped uniformly to allow both bulk and surface characterization. The silicon content was measured prior to growth with a mass spectrometer at the substrate's growth position. Following growth, the silicon density in heavily doped layers was verified by electron microprobe. Bulk carrier concentrations and mobilities were measured by Hall effect. Surface space-charge density was inferred from the specific contact resistivity of nonalloyed metallurgy applied *in situ* following growth. Ag was chosen for its lack of reaction with GaAs and ease of patterning into transmission lines.<sup>6</sup> Actual contact spacings, measured by optical microscopy, were the major source of uncertainty in the resistivity measurement. Surface space-charge density was estimated by reference to the work of Chang *et al.*<sup>7</sup> and Schroder and Meier.<sup>8</sup> For an effective mass  $m^*$ , Richardson constant  $A^{**}$ , Boltzmann constant  $k$ , temperature  $T$ , Planck's constant  $h$ , a net space-charge density  $(N_D - N_A)$  of  $N$ , electron charge  $q$ , permittivity  $\epsilon$ , and barrier  $\Phi$ , the specific contact resistivity  $\rho_c$  is

$$\rho_c \simeq (k/qTA^{**}) \exp \left[ \frac{2\pi\Phi}{h} \sqrt{\frac{\epsilon m^*}{N}} \right].$$

The barrier  $\Phi$  is reduced from the low-field barrier height  $\phi$  by  $\sqrt[4]{q^3 N \phi / 8\pi^2 \epsilon^3}$ . This expression for  $\rho_c$  is approximate, and the temperature dependence of the pre-exponential factor is uncertain.

Bulk electron concentrations appear in Fig. 1 as triangular symbols. Up to  $\sim 10^{19} \text{ cm}^{-3}$ , the electron density is nearly equal to the silicon density, as noted by others,<sup>5,9</sup> from mobilities similar to nonamphoteric dopants.<sup>10</sup> Electron density did not vary detectably with substrate temperature, arsenic species, or arsenic pressure, although Ga-rich growth was not examined. Observed variations<sup>9</sup> may be due to unintentional impurities.<sup>11</sup> At silicon densities above  $\simeq 10^{19} \text{ cm}^{-3}$ , the electron concentration peaks and drops to a level dependent upon substrate temperature.

The theoretical and actual values of  $\rho_c$  are presented in Fig. 2. The square symbol shows the result of Barnes and Cho<sup>12</sup> for Sn doping. The measured values of  $\rho_c$  for the *in situ* Ag contacts are plotted versus silicon density using circles. Silicon densities of 0.4, 1, and  $2 \times 10^{20} \text{ cm}^{-3}$  yield  $\rho_c$  of

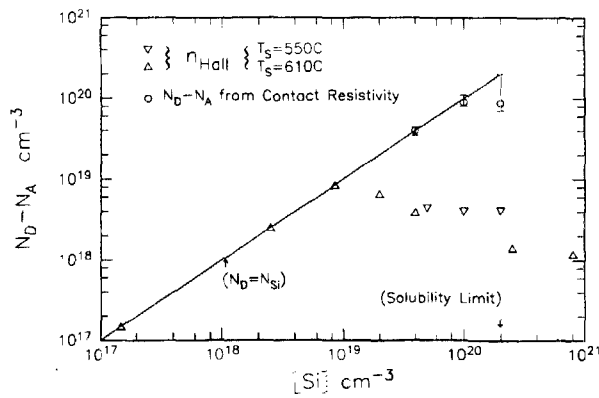


FIG. 1. Electron density and surface space-charge density of MBE (100) GaAs is plotted vs silicon concentration. The Hall electron density is shown for layers grown at 550 ( $\nabla$ ) and 610  $^{\circ}$ C ( $\Delta$ ). The surface space-charge density inferred from the specific resistivity of nonalloyed contacts (O) is shown from Fig. 2.

$5 (\pm 2)$ ,  $1.3 (\pm 0.7)$ , and  $1.5 (\pm 1) \mu\Omega \text{ cm}^2$ , respectively. Within the accuracy of both measurement and theory, the resistivities obtained correspond with the theoretical values for a 0.7–0.8-eV barrier if the silicon density and the space-charge density are equivalent. The lowest resistivity indicates a space-charge density of  $\approx 1 \times 10^{20} \text{ cm}^{-3}$ , which exceeds the highest electron concentration obtained in GaAs with any dopant<sup>12</sup> and exceeds by tenfold the maximum electron density obtained in bulk GaAs with Si doping.

The effects of native oxide formation due to air exposure confirmed the presence of a high space-charge density layer confined to the near-surface region. Cr was evaporated following an HCl rinse of layers that had been exposed to air for several days. A layer with a Si density of  $5 \times 10^{19} \text{ cm}^{-3}$  yielded  $\rho_c = 22 (\pm 2) \mu\Omega \text{ cm}^2$ , several times that expected for a similar *in situ* contact. The resistance of any residual oxide only partly explains the increased  $\rho_c$ , because higher Si densities produced  $\rho_c$  above  $100 \mu\Omega \text{ cm}^2$ , typical of bulk Si doping limits. If high space-charge density exists only within the original surface depletion zone, then oxidation of the top few nanometers of GaAs extends the depletion zone into low space-charge density material, increasing  $\rho_c$ . For the  $5 \times 10^{19} \text{ cm}^{-3}$  Si density, oxidation consumes some of the high space-charge density layer, yielding  $\rho_c$  lower than bulk doping yields but higher than a similar *in situ* contact. At higher silicon densities, all of the high space-charge density layer is destroyed, exposing bulk material that exhibits high contact resistivity.

Silicon can be a donor or acceptor in GaAs. At equilibrium, the ratio of donors to acceptors is given by the expression

$$N_D/N_A = \text{Si}_{\text{Ga}}/\text{Si}_{\text{As}} = k(T) \times (p/n) \times P_{\text{As}_2}, \quad (1)$$

where  $N_D$  and  $N_A$  are the donor and acceptor concentrations,  $k(T)$  is a temperature-dependent constant incorporating the equilibrium arsenic pressure over GaAs,  $p/n$  is the carrier concentration ratio, and  $P_{\text{As}_2}$  is the arsenic dimer pressure. At a given temperature and arsenic pressure, if the GaAs is intrinsic, the ratio of donors to acceptors is constant because  $p/n \approx 1$ . MBE of GaAs commonly uses an excess As flux, yielding a  $c(2 \times 4)$  reconstruction, which Katnani *et*

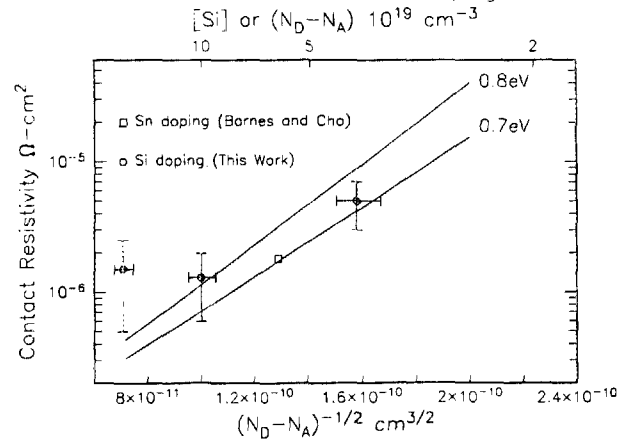


FIG. 2. Specific contact resistivity  $\rho_c$  for nonalloyed ohmic contacts to  $n$ -GaAs is plotted vs the reciprocal square root of the space-charge density. The lines show theoretical (see Refs. 7, 8)  $\rho_c$  for 0.7- and 0.8-eV barriers. ( $\square$ ) The result of Barnes and Cho (see Ref. 12) showing the accuracy of the theory. ( $\circ$ )  $\rho_c$  for our contacts with [Si] substituted for space-charge density. The agreement with theory shows that surface space-charge density in these samples is equivalent to the silicon density.

*al.*<sup>13</sup> show yields  $E_c - E_f \approx 0.8 \text{ eV}$ . Free electrons are depleted from the surface region, where initial dopant site selection occurs. In this depletion region, the  $p/n$  ratio is near 1 and, therefore, in this region the equilibrium  $N_D/N_A$  should be that of intrinsic material even though the bulk may be extrinsic. Therefore, for conditions that create low-compensation  $n$ -type material at low dopant concentration, the surface equilibrium  $N_D/N_A$  should be large for any dopant concentration.

Kinetic factors are expected to prevent equilibration in MBE. However, the typical micron-scale surface mobility of Ga adatoms and the low density of stoichiometric defects in MBE GaAs show that surface kinetics may allow some reactions to reach equilibrium. At high silicon concentrations, initially depleted GaAs with high  $N_D/N_A$  encounters bulk conditions as more material is grown atop it. To reach bulk equilibrium where  $N_D/N_A$  is near 1, up to nearly half the silicon atoms must switch from donor to acceptor sites. The Ga vacancies and As interstitials produced must diffuse to the surface for site switching to continue. Their diffusivity is enhanced by proximity to the surface by exponentially increasing near-surface vacancy concentrations and linearly increasing concentration gradients. Therefore, the kinetics of site switching can approach surface rates at high silicon concentrations because the high space-charge density shrinks the surface depletion layer so that bulk electron concentrations occur only a few nanometers from the surface. The kinetic barrier to equilibration can be seen in Fig. 1, where the electron density peaks near  $10^{19} \text{ cm}^{-3}$ . Increasing the Si density shrinks the surface depletion layer, increasing site switching so that the electron density drops to its temperature-dependent maximum equilibrium value.

The low contact resistances obtained ( $1.3$ – $5 \mu\Omega \text{ cm}^2$ ) are inconsistent with the bulk doping behavior of silicon in GaAs. However, Miller *et al.*<sup>4,5</sup> also used silicon doping at high concentrations for MBE tunnel diodes and obtained unexpectedly high conductances. Both their diodes and our contacts have Si-doped GaAs that is depleted of free elec-

trons during growth due to the  $p$ - $n$  junction and surface potentials. Among alternative explanations, a deep donor at high density would yield both a high space-charge density and low electron density, but it is unlikely that the deep level would be as tightly confined to the surface region as the air-exposure experiments indicate. Similarly, a substantial reduction of  $\Phi$  would cause low  $\rho_c$  despite the low bulk electron concentration, but then the increase in  $\rho_c$  with increasing Si density for the air-exposed samples is unexplained. Thus, high space-charge density in the surface depletion region is the likely mechanism by which the low contact resistivity is obtained.

In conclusion, *in situ* Ag metallization of MBE GaAs doped at  $1 \times 10^{20} \text{ cm}^{-3}$  with Si yields a nonalloyed specific contact resistivity of  $1.3 \mu\Omega \text{ cm}^2$ . This result indicates a space-charge density in the GaAs at the metal interface approximately equal to the silicon density, despite a bulk electron density of  $4 \times 10^{18} \text{ cm}^{-3}$ . This effect is explained by midgap Fermi-level pinning of the arsenic-stabilized GaAs surface during growth. Silicon's solubility in GaAs is  $\approx 2 \times 10^{20} \text{ cm}^{-3}$ , suggesting that nonalloyed contacts applied *in situ* could yield a specific contact resistivity as low as  $0.5 \mu\Omega \text{ cm}^2$ .

The authors gratefully acknowledge N. Braslan for helpful discussions and A. Boulding, F. Cardone, and R. Savoy for microprobe analysis.

- <sup>1</sup>R. L. Longini and R. F. Greene, Phys. Rev. **102**, 992 (1956).
- <sup>2</sup>M. E. Greiner and J. F. Gibbons, Appl. Phys. Lett. **44**, 750 (1984).
- <sup>3</sup>P. D. Kirchner, J. M. Woodall, and S. L. Wright, Abstract in IEEE Trans. Electron Devices **ED-30**, 1590 (1983).
- <sup>4</sup>D. L. Miller, S. W. Zehr, and J. S. Harris, Jr., J. Appl. Phys. **53**, 744 (1982).
- <sup>5</sup>D. L. Miller, H. T. Yang, and S. W. Zehr, "Cascade AlGaAs-GaAs Solar Cell Research using MBE," Los Angeles SPIE Technical Symposium, SPIE Proceedings, 1982, p. 323.
- <sup>6</sup>H. H. Berger, J. Electrochem. Soc. **119**, 509 (1972); Solid State Electron. **15**, 145 (1972).
- <sup>7</sup>C. Y. Chang, Y. K. Fang, and S. M. Sze, Solid State Electron. **14**, 541 (1971).
- <sup>8</sup>D. K. Schroder and D. L. Meier, IEEE Trans. Electron Devices **ED-31**, 637 (1984).
- <sup>9</sup>Y. G. Chai, R. Chow, and C. E. C. Wood, Appl. Phys. Lett. **39**, 800 (1981).
- <sup>10</sup>J. De-Sheng, Y. Makita, K. Ploog, and H. J. Queisser, J. Appl. Phys. **53**, 999 (1982).
- <sup>11</sup>R. A. A. Kubiak and E. H. C. Parker, Appl. Phys. A **35**, 75 (1984).
- <sup>12</sup>P. A. Barnes and A. Y. Cho, Appl. Phys. Lett. **33**, 651 (1978).
- <sup>13</sup>A. D. Katnani, P. Chiaradia, H. W. Sang, Jr., and R. S. Bauer, J. Vac. Sci. Technol. B **2**, 471 (1984).

## $NpnN$ double-heterojunction bipolar transistor on InGaAsP/InP

L. M. Su,<sup>a)</sup> N. Grote, R. Kaumanns, and H. Schroeter

Heinrich-Hertz-Institut für Nachrichtentechnik Berlin GmbH, Einsteinufer 37, D-1000 Berlin, 10, West Germany

(Received 20 November 1984; accepted for publication 10 April 1985)

Double-heterojunction bipolar transistors have been fabricated on InGaAs(P)/InP with current gains of up to 200. Transistors with a  $p^+$ -InGaAs/ $N$ -InP base/collector junction exhibited drastic gain reduction at low collector bias voltages which is ascribed to the electron repelling effect of the conduction-band spike formed at the collector heterojunction. To overcome this complication a thin  $n$ -InGaAs transition layer was inserted between the ternary base and the InP wide-gap collector. The resulting  $nN$  double-layer collector structure leads to excellent current/voltage characteristics.

In the last few years, III-V compound heterojunction bipolar transistors (HBT) have gained increasing interest for microwave amplification and high-speed switching as well as for optical detection. Microwave HBT's on GaAlAs/GaAs have already been reported with excellent high-frequency properties, namely, unity gain cut-off frequencies of up to 25 GHz.<sup>1-3</sup> HBT's on InGaAsP/InP, however, have been mostly developed as phototransistors (e.g., Refs. 4 and 5) for long wavelength (1-1.6  $\mu\text{m}$ ) optical communication applications. Only recently InP-based "electrical" bipolar transistors with base terminals have been published. These devices mainly comprise a base-collector homojunction of InGaAs ( $x_{\text{In}} = 0.53$ ).<sup>6-8</sup> Moreover, double-heterojunction

transistors employing an InP wide gap collector in conjunction with a quaternary InGaAsP ( $\lambda_g = 1.1 \mu\text{m}$ ) base layer have been fabricated to form a driving circuit together with a monolithically integrated laser diode providing 1.6 Gbit/s modulation capability.<sup>9</sup>

In order to optimize the high-frequency performance of InGaAsP/InP HBT's a device structure should be chosen which uses an  $\text{In}_{0.53}\text{Ga}_{0.47}\text{As}$  layer for the base and InP as a wide gap collector.  $\text{In}_{0.53}\text{Ga}_{0.47}\text{As}$  is known to exhibit the highest electron mobilities ( $\mu_{300\text{K}} \approx 8-11 \times 10^3 \text{ cm}^2/\text{Vs}$  at  $n \approx 10^{16} \text{ cm}^{-3}$ ) within the InGaAsP/InP alloy system, which result in short transit times in the (neutral) base. On the other hand, for the collector of a microwave transistor the high-field drift velocity rather than the (low field) mobility is of importance. This is because the drift velocity deter-

<sup>a)</sup> On leave from Peking Electron Tube Factory, Peking, China.